European Conference on Optical Communication (ECOC) 2022 © Optica Publishing Group 2022

Demonstration of continuous multiple access with image-rejection coherent receiver and DML transmitters

Jeison Tabares(1,2), Miquel Masanas(1), Ivan Cano(3) and Josep Prat(1)

(1) Department of Signal Theory and Communications, Universitat Politècnica de Catalunya, 08034, Barcelona, Spain
(2) Luxquanta Technologies, Carl Friedrich Gauss 3, 08860, Castelldefels, Spain
(3) Munich Research Centre, Huawei Technologies
miquel.masanas@upc.edu

Abstract *We demonstrate a UD-WDM PON using DML transmitters with multilevel intensity modulation, both in base-band and RF, and a spectrally-efficient heterodyne receiver. We provide comparison with a homodyne receiver. Two users at the same IF are detected simultaneously avoiding image frequency interference while minimizing complexity. ©2022 The Author(s)*

Introduction

Optical local area networks can find applications for industrial and critical machine communications as they offer high reliability and robustness against electromagnetic interference. Also, IoT networks can have a high number of terminals like sensors and actuators which might not transmit a high speed but need low and deterministic latency [1-3]. To reduce the cost of the network, a point-to-multipoint architecture can be used [4]. In addition, the transceivers should be simple to keep the footprint and complexity as low as possible. To address these requirements, coherent-lite schemes might be a key-enabling technology as they enhance the optical power budget and allow for filter-less ultra-dense wavelength division multiplexing (UD-WDM) which can bring significant latency reduction and reliability.

In this work, we propose continuous multiple access (CMA) implemented with cost-effective user equipment. We use conventional low-cost directly modulated lasers (DMLs) with thermo-electric cooling for wavelength (λ) tuning, as optical transmitters (TX). At the receiver (RX), placed at the central aggregation point of the network, we use polarization-independent heterodyne detection with image-frequency cancellation, to simultaneously detect two users at both sides of the local oscillator (LO), thus doubling the spectral efficiency and lowering the needed electrical bandwidth (BW) of the RX. For the tests, we directly modulated NRZ and PAM-4 both in base-band (BB) and over RF. The modulation rates were 625 MBd and 1.25 GBd for RF and BB respectively, reaching up to 1.25 and 2.5 Gb/s optical access links. We achieved users separation as low as 2.3 GHz with RX sensitivities better than -30 dBm.

Network architecture

For simultaneous detection of two BB or RF users, the heterodyne image-rejection (IR) RX implements the optical front-end shown in Fig. 1. The details of the polarization recovery and IR are provided in [5]. The first network scenario, illustrated in Fig. 2a, uses λ-to-the-user with BB modulation. Two adjacent WDM users are separated by $\Delta\lambda = 2\mathrm{IF}$, where IF is the intermediate frequency of the heterodyne detection.

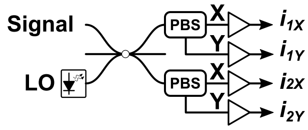

Fig. 1: 3x3 heterodyne image-rejection RX front-end.

The second scenario, depicted in Fig. 2b, considers electrical frequency division multiplexing (FDM). Several network users share a single λ, and their data are modulated into different RF frequencies. This scenario is studied using two different coherent detection schemes (see Fig. 2b inset): (I) the novel heterodyne RX with IR by placing the LO in middle of two RF users, and (II) the conventional homodyne RX with the LO matched to the central emitted λ and band-pass filters separating the individual RF users.

Experimental results

The two different scenarios were tested using NRZ and PAM-4. In all tests, the modulation index was 0.6, and we shaped the pulses with a raised-cosine filter having a roll-off of 1. The modulation index was experimentally optimized to balance the trade-off between high RX sensitivity and low modulated spectral width due to laser chirp spreading. The PAM-4 was equalized at the RX with a 4-tap FIR filter to compensate for non-ideal components and channel response, including electro-optical hardware. The optical link implemented 25 km of SSMF and the data detection and users demultiplexing at the RX was carried out by a 50 GSa/s real-time oscilloscope. For comparison, we also report single-user measurements for each scenario, detected with the homodyne RX.

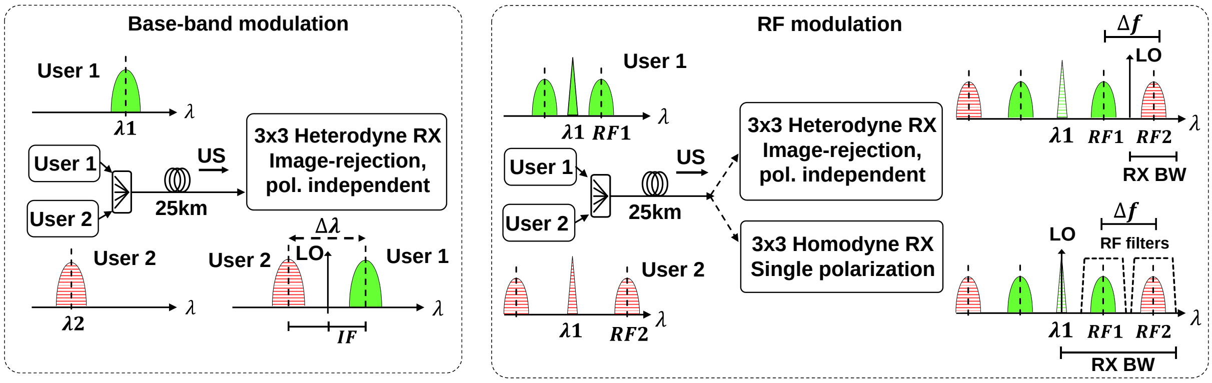

(a) (b)

Fig. 2: (a) CMA access with two UD-WDM users modulated in BB and detected simultaneously by the 3x3 heterodyne IR RX**; (b)** Idem but using FDM users modulated on RF carriers, and with two coherent detection techniques: the novel 3x3 heterodyne RX with IR, and conventional homodyne RX.

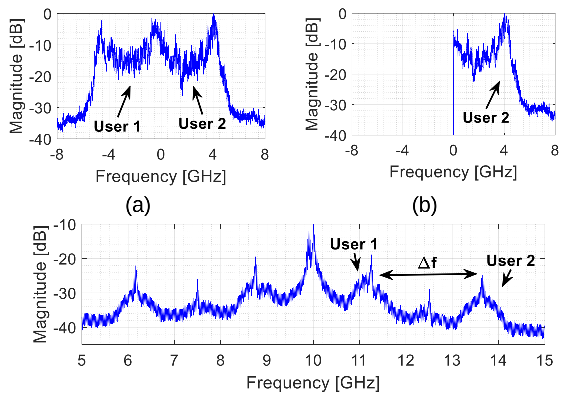

(c)

Fig. 3: Electrical spectrum of two users after photodetection: **(a)** both users modulated in BB with NRZ at 1.25 Gb/s; **(b)** User 2 after cancellation of User 1 by the heterodyne IR RX; **(c)** two PAM-4 users modulated in RF at 1.25 Gb/s (spectrum centered at 10 GHz).

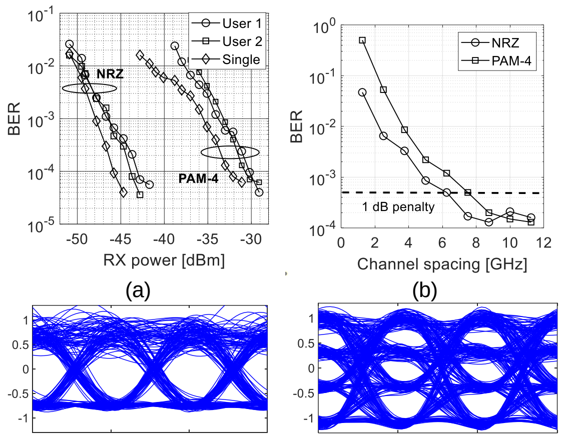

Fig. 4: For two users at 1.25 GBd with NRZ and PAM-4 in BB, detected simultaneously by the 3x3 heterodyne IR RX: **(a)** BER vs. RX power; **(b)** BER vs. channel spacing, the LO is placed in middle of the two users ($\Delta\lambda = 2IF$). Detected eye diagram error-free for **(c)** NRZ and **(d)** PAM-4.

a) UD-WDM with dedicated λ per user and BB modulation.

In the UD-WDM scenario in Fig. 2a, each user modulated BB data at R_B = 1.25 GBd, both NRZ and PAM-4. The IF was initially set to $2R_B$ = 2.5 GHz, hence $\Delta\lambda$ = 5 GHz. The detected electrical spectrum at the RX after simultaneous detection of User 1 and User 2 is plotted in Fig. 3a for NRZ at 1.25 Gb/s. The plotted spectrum corresponds to the recovered complex *I+jQ* signal for each polarization. Note that the modulated spectral width is significantly larger than R_B because of the laser chirp spreading. Fig. 3b shows the spectrum after IR to cancel the interference from User 1, with more than 40 dB of rejection.

The BER performance of the two users detected simultaneously by the same 3x3 heterodyne RX with IR is reported in Fig. 4a. The bit rates are 1.25 and 2.5 Gb/s for NRZ and PAM-4 respectively, IF = 2.5 GHz, and user separation $\Delta\lambda$ = 5 GHz. Notably, the two users show similar performances after simultaneous detection, for both modulation formats. The RX sensitivities at BER = 10^{-3} are -46 and -34 dBm for NRZ and PAM-4 respectively, which are 2 and 1.5 dB worse than the single-user tests. These results very well match the results in [6] with NRZ using DMLs. The sensitivity penalty at 10^{-3} BER for PAM-4 with respect to NRZ, with $\Delta\lambda$ = 5 GHz, is about 12 dB.

Next, the channel spacing was experimentally evaluated and the results are plotted in Fig. 4b, in terms of the BER as a function of the λ spacing between two users. It is worth mentioning that $\Delta\lambda = 2\mathrm{IF}$ for simultaneous detection of two users by the same heterodyne RX. The results indicate that the minimum channel spacing for 1 dB penalty at BER = 10^{-4} is about 6.5 and 7.5 GHz for NRZ and PAM-4 respectively, at 1.25 GBd.

b) FDM through RF subcarrier modulation, shared λ for several users.

In the second scenario, two users emitted at the same λ and were multiplexed in electrical FDM through RF modulation of the lasers, as shown in Fig. 3b. The users modulated NRZ and PAM-4 data at 625 MBd, first on RF carriers at 1.25 and 3.75 GHz for User 1 and User 2 respectively. The RF frequencies were later varied to evaluate the minimum FDM channel separation Δf.

At the RX side two coherent detection schemes were evaluated. On the one hand, the 3x3 homodyne RX, single-polarization. The LO was tuned at the same λ than the two TXs, then the RF User 1 and User 2 were demultiplexed by electrical band-pass filters. On the other hand, the two users were detected by the 3x3 heterodyne IR RX, polarization-independent, by locating the LO in middle of two RF users, as illustrated in Fig. 2b; in this case, the users demultiplexing was carried out by the image-rejection part of the RX DSP.

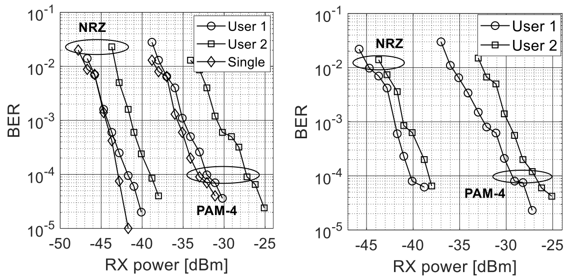

(a) (b)

Fig. 5: BER vs. RX power for two FDM users at 625 MBd with NRZ and PAM-4, detected simultaneously by **(a)** the 3x3 homodyne RX and **(b)** the 3x3 heterodyne IR RX.

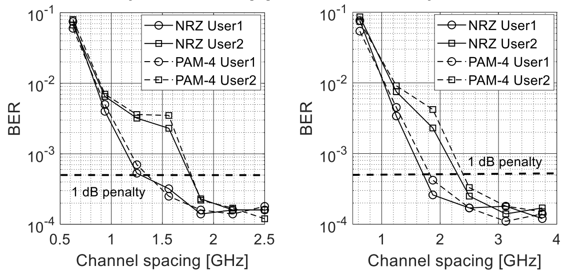

(a) (b)

Fig. 6: BER vs. RF user separation for NRZ and PAM-4 at 625 MBd, detected by **(a)** 3x3 homodyne RX and **(b)** 3x3 heterodyne image-rejection RX. The RF of User 1 is fixed at 1.25 GHz and the RF of User 2 is swept to evaluate Δf.

The BER performances are reported for the homodyne and heterodyne IR RXs, in Fig. 5a and 5b respectively. At BER = 10^{-3}, and considering first the User 1 at RF = 1.25 GHz, the 3x3 homodyne RX performed better, with RX sensitivity of -44.5 and -35 dBm for NRZ and PAM-4 respectively. The sensitivity penalty for the 3x3 heterodyne IR RX for the same User 1 was 2.5 and 3 dB for NRZ and PAM-4 respectively. In theory, the IR compensates the 3 dB penalty in sensitivity of heterodyne detection compared with homodyne, owing to the cancelation of half the total noise BW. In the experiment, however, we found lower sensitivity for the 3x3 heterodyne RX due to extra insertion losses of the optical front-end, compared with the single-polarization homodyne RX. The sensitivity penalty between NRZ and PAM-4 at the same R_B was of 9.5 and 10 dB for the homodyne and the heterodyne RX respectively, considering User 1. For the User 2 at RF = 3.75 GHz, detected by the homodyne RX, the sensitivity penalty at BER = 10^{-3} with respect to User 1 was 3 and 4 dB for NRZ and PAM-4 respectively. Interestingly, the penalty between User 1 and User 2 with the same modulation format, is lower in the heterodyne IR RX, of about 1 and 2 dB for NRZ and PAM-4 respectively, mostly due to the lower required RX BW to detect the two users; thus, the total noise BW is lower and non-ideal frequency responses at higher frequencies have less impact.

The final tests evaluated the required RF user separation Δf. For the test, User 1 was fixed at RF = 1.25 GHz, then the RF frequency of User 2 was swept to evaluate the minimum Δf for 1 dB penalty at BER= 10^{-4}. Both users were detected simultaneously during the tests. The results are plotted in Fig. 6a for homodyne and 6b for heterodyne RX. Interestingly, the curves for RF User1 and User 2 are asymmetrical in all cases because, for Δf = 1.25 GHz, the User 2 overlaps the 2nd harmonic of the modulated User 1 (see Fig. 3c), producing a penalty at the detection of User 2 but not in User 1. Taking as reference the largest RF separation required by the User 2, the minimum Δf for 1 dB penalty is 1.75 and 2.3 GHz for homodyne and heterodyne RX respectively, which represents 30% larger RF users spacing due to the heterodyne detection, however, the heterodyne IR RX requires 52% less RX BW than the homodyne RX. Moreover, by comparing the required separation between RF users in Fig. 6 with respect to the BB users in Fig. 4b), one note that for BB users at 1.25 GBd the user separation is $\Delta\lambda > 5R_B$. In contrast, for RF users at 625 MBd the RF separation is $\Delta f > 4R_B$, lower than in BB modulation because of the narrower modulated spectral width, mainly dictated by the laser chirp.

Conclusion

We demonstrated simultaneous CMA using intensity modulation of low-cost DMLs with a novel polarization-independent, spectrally efficient heterodyne RX. The image-rejection of the heterodyne RX allowed to use the same electrical BW to demodulate two users. The obtained results indicated that multiplexing the users in electrical RF required adjacent users separation of $\Delta f > 4R_B$, less than the separation required in λ multiplexing with baseband modulation, that needed $\Delta\lambda > 5R_B$ due to the laser chirp spectral spreading, which affects more in base-band than in RF modulation.

References

[1] L. Antão, R. Pinto, J. Reis and G. Gonçalves, "Requirements for Testing and Validating the Industrial Internet of Things," *2018 IEEE International Conference on Software Testing, Verification and Validation Workshops (ICSTW)*, 2018, pp. 110-115, doi: 10.1109/ICSTW.2018.00036.

[2] N. Brahmi, O. N. C. Yilmaz, K. W. Helmersson, S. A. Ashraf and J. Torsner, "Deployment Strategies for Ultra-Reliable and Low-Latency Communication in Factory Automation," 2015 IEEE Globecom Workshops (GC Workshops), 2015, pp. 1-6,

[3] Ernst & Young, "White paper: The backbone of digital economies: the revolution of global industries through optical communications" (2021)

[4] D. Welch *et al*., "Point-to-Multipoint Optical Networks Using Coherent Digital Subcarriers," in *Journal of Lightwave Technology*, vol. 39, no. 16, pp. 5232-5247, 15 Aug.15, 2021, doi: 10.1109/JLT.2021.3097163.

[5] J. Tabares and J. Prat, "Low-Complexity Phase-and-Polarization-Diversity Coherent Receiver with High Spectral Efficiency for UDWDM," in *Proc. Opt. Fiber Commun. Conf. Exhib.*, 2021 (OFC), Paper Th5I.2.

[6] M. Presi, R. Corsini, M. Artiglia, E. Ciaramella, " Using directly modulated DFBs without power penalty in low-cost and high-power budget coherent access networks" *in Electronics Letters, vol. 50, no 7, pp 536-538.* DOI: